Band Bending in Mg-Colored and O-2-Activated Ultrathin MgO(001) Films

Thomas Jaouen, Baptiste Hildebrand, Philipp Aebi, Gabriel Delhaye, Sylvain Tricot, Bruno Lépine, Guy Jezequel, Philippe Schieffer

Band Bending in Mg-colored and O_2-activated Ultrathin MgO(001) Films

T. Jaouen, [†,¶] B. Hildebrand, [†] P. Aebi, [†] G. Delhaye, [‡] S. Tricot, [‡] B. Lépine, [‡] G. Jézéquel, [‡] and P. Schieffer [*,‡]

†*Département de Physique and Fribourg Center for Nanomaterials, Université de Fribourg, CH-1700 Fribourg, Switzerland*

‡*Département Matériaux et Nanosciences, Institut de Physique de Rennes UMR UR1-CNRS 6251, Université de Rennes 1, F-35042 Rennes Cedex, France*

¶*Corresponding author*

E-mail: thomas.jaouen@unifr.ch

Abstract

Ultrathin MgO films grown on Ag(001) have been investigated using x-ray and ultraviolet photoemission spectroscopies for oxide films successively exposed to Mg and O_2 flux. Studying work functions and layer-resolved Auger shifts allows to keep track of band profiles from the oxide surface to the interface and reveal the charge transfer mechanisms underlying the controlled creation of Mg-induced surface color centers and the catalytic enhancement of O_2 activation. Our results demonstrate that one can intimately probe the catalytic properties of metal-supported ultrathin oxide films by studying the electronic band alignment at interfaces.

February 15, 2017

Introduction

Metal-supported ultrathin oxide films have been widely studied both experimentally and theoretically in the field of heterogeneous catalysis due to their pivotal role in controlling charging mechanisms, adsorption properties, and catalytic activation of metal ad-atoms and molecules.[1–6] The favored electron tunneling through the oxide film brought by the ultrathin limit opens new catalytic pathways for charge transfer mechanisms as demonstrated by the charging of Au atoms and the spontaneous activation of carbon monoxide and molecular oxygen upon adsorption on ultrathin MgO(001) films.[4,5,7–9]

The catalytic properties of metal-supported ultrathin oxide films are also strongly impacted by the presence of defects. For example, depositing metal adatoms on oxides is known to boost the reactivity via electron transfer to adsorbed molecules.[10] It has been further shown that metal clusters deposited on defect-rich MgO films were catalytically more active than the stoechiometric oxide.[11–14] Theoretical calculations have provided strong support that this was related to neutral and singly charged oxygen vacancies at the surface of MgO, also known as the F_s and F_s^+ surface color centers.[15,16]

Therefore, ultrathin, colored oxide films can in principle allow reaching optimal catalytic properties. However, the design of such advanced catalytic devices is not only facing the complexity of ultrathin limit and controlled defect generation but also requires a detailed knowledge of electronic structures at interfaces that can host a variety of entangled charge transfer mechanisms. Recent electron paramagnetic resonance (EPR) experiments have reported the ability of producing F_s^+ color centers on 20 ML-thick MgO(001) single crystalline films by deposition of small amounts of Mg at low temperatures.[17] These centers have been attributed to unpaired electrons trapped at morphological defects of the MgO surface in contrast to color centers prepared by electron bombardment that originate in electron trapping within oxygen vacancies.[18]

In this paper, we report spectroscopic evidence for controlled creation of Mg-induced color centers on *ultrathin* MgO films grown on Ag(001). We further show that they serve as host for subsequent O_2 activation by favoring superoxide O_2^- anions formation . The associated charge transfer mechanisms are identified by using x-ray and ultraviolet photoemission spectroscopy (XPS-UPS) for monitoring, layer-by-layer, the impact of Mg and O_2 treatments on the electronic band profiles, i.e. on band bending.

Experimental methods

All experiments were performed in a multi-chamber ultrahigh vacuum (UHV) system with base pressures below 2×10^{-10} mbar. A molecular beam epitaxy chamber equipped with reflection high-energy electron diffraction (RHEED) is interconnected with XPS-UPS analysis chamber via a transfer chamber. The (001)-oriented Ag single crystal was cleaned by several cycles of Ar^+ ion bombardment and annealing at 670-720 K during 30 min. The cycles were repeated until a good RHEED pattern and a reproducible work function resulted. The final stable value of the work function of Ag(001) was $\phi_m = 4.38\pm0.05$ eV. The 3 monolayers (ML) thick MgO films (one monolayer is defined as one half MgO lattice parameter, i.e. 1ML =

2.105 Å) were grown on the prepared Ag(001) surface by evaporation of Mg in O_2 background atmosphere (oxygen pressure = 5×10^{-7} mbar) at 453 K with a cube-on-cube epitaxy with respect to the Ag(001) substrate. The Mg (2.4×10^{13} atoms/(cm^{2}s)) and O_2 post-exposures have been performed at a substrate temperature of 513 K and 300 K, respectively.

The measurements were carried out using XPS and UPS measurements. The kinetic energy of the emitted electrons has been measured by employing a hemispherical analyzer (Omicron EA125) with a five-channels detection system. Al $K\alpha$ was used as the x-ray source and He-I resonance ($h\nu$ =21.22 eV) line provided the UPS source for photoemission experiments. The total energy resolutions were respectively 0.80 and 0.15 eV for XPS and UPS. The work function of the dielectric system (ϕ_m^*), defined as the energy of the vacuum level (E_{Vac}) with respect to the Fermi level of the MgO/Ag(001) system (E_F), is determined from the low-energy cutoff (E_{cut}) of the secondary photoelectron emission: $\phi_m^* = h\nu - (E_F - E_{cut})$. To this end, the samples were biased at -8 V to make the measurements of the very low-energy region of the spectrum reliable.

Results and discussion

In Fig. 1 are shown the variations of the work function ($\Delta\phi$) and of the MgO-valence band position (ΔVB) as a function of the Mg exposition time for two samples consisting of 3 and 5 ML of MgO grown on Ag(001). The methods used for the determination of the work function and valence band (VB) position extracted from our UPS spectra are given in Ref.[19] The semi-logarithmic representation together with the comparison of the energy shifts obtained for the 3 and 5 ML-thick samples allows to highlight a two-step evolution of the considered quantities as a function of the Mg exposure time. Whereas during the first 20 seconds the work function shifts are the same for 3 and 5 ML and about two times higher than the VB shifts, further exposition to Mg leads to similar changes of $\Delta\phi$ and ΔVB but whose magnitude is highly dependent on the MgO thickness. For 5 ML, the shifts observed

after 720 seconds of Mg exposure reach ∼-0.25 eV, i.e. two times lower than those obtained for the 3 ML-thick sample.

Thus, our observations reveal two distinct regime in the Mg diffusion and adsorption mechanisms as a function of, both, the Mg flux and the MgO thickness. Since in the first phase $\Delta\phi$ and ΔVB show the same variations and values irrespective of the MgO thickness, we conclude that we are facing a surface mechanism. The measured $\Delta\phi$ essentially reflects a band bending effect resulting from a positive charge accumulation at the surface of the dielectric layer.

In the second phase, between 40 and 720 s of Mg exposures, we observe similar changes of $\Delta\phi$ and ΔVB for both the 3 ML and 5 ML-thick samples thus demonstrating that the Fermi level pinning position progressively changes at the MgO/Ag(001) interface. As discussed in Ref.,[20] this is driven by the Mg atoms incorporation at the MgO/Ag(001) interface. Note that, in this phase, the variation of the valence band and work function for 3 ML is twice the one observed for 5ML-MgO. This thickness dependence suggests that the probability that an Mg atom reaches the MgO/Ag(001) interface is inversely proportional to the film thickness.

Figure 2 shows the low-energy cutoff of the secondary photoelectrons emission (Fig. 2(a)), the He-I UPS spectra of the valence band (Fig. 2(b)), and the Al $K\alpha$ spectra of the Mg $1s$ and O $1s$ core levels (Fig. 2(c)) for the MgO(3ML)/Ag(001) sample and after successive exposures to a Mg and O_2 flux. The Mg and O_2 exposures have been performed during 20 s and 240 s, respectively. The energy reference is E_F, the low-energy cutoff positions is taken at the maximum slope of their rising edges and the MgO valence band maximum (VBM), is obtained via a linear extrapolation of the leading edge of the valence band (VB) spectrum, [19] that consists of overlapped MgO O$2p$ states (main structures at 4.5 eV and 8 eV) and Ag $4d$ states of the metal substrate (around 4.5 eV).[21] The Mg flux exposure leads to a work function reduction of the metal/oxide system by 0.37 ± 0.05 eV (Fig. 2(a)) and to a VBM shift of 0.16± 0.10 eV towards higher binding energy (Fig. 2(b)) in close agreement with the Mg $1s$ (-0.20 ± 0.05 eV) and O$1s$ (-0.20 ± 0.05 eV) core-level kinetic energy shifts (red

lines Fig. 2(c)). As we can see, further exposures to O_2 now reveals that the work-function shifts can be inverted ($+0.23 \pm 0.05$ eV), and the VBM ($+0.16 \pm 0.05$ eV) and core-level shifts ($+0.20 \pm 0.05$ eV and $+0.16 \pm 0.05$ eV for Mg $1s$ and O$1s$, respectively) fully canceled.

Let us now focus on the evolution of the Mg $KL_{23}L_{23}$ Auger emission through the different surface treatments. For 3 ML of MgO, the Mg $KL_{23}L_{23}$ Auger transition is indeed a very powerful spectroscopic probe thanks to its layer-by-layer resolution originating in image potential screening at the metal/oxide interface. [20] It has been for example exploited to access, *layer-by-layer*, the atomic structure of MgO ultrathin films, [22] as well as the unoccupied interface and surface states of the MgO/Ag(001) system. [23]

In the present study, the layer-resolved Mg $KL_{23}L_{23}$ Auger emission further allows to keep track of band profiles from the oxide surface to the interface. Figure 3(a) shows normal-emission Mg $KL_{23}L_{23}$ Auger spectra (vertically shifted for clarity) of the 3 ML MgO sample before and after exposition to the Mg atomic flux. Figure 3(b) then compares the Auger spectra obtained after Mg (top spectrum) and O_2 (bottom spectrum) exposures. The 3 ML reference spectrum is fitted by three Auger components C_1, C_2, and C_3, with maxima situated at 1179.1 eV, 1177.8 eV, and 1176.8 eV and which correspond to Auger electron emission from the first, second and third MgO plane above the metal-oxide interface.

The band bending induced by an Mg exposure of 20 s is clearly revealed in Fig. 3(a) through the evolution of the C_1, C_2, and C_3 positions. The interface component shows no shift after Mg exposure whereas C_2, and C_3 have lowered kinetic energies by 0.16 and 0.32 eV, respectively. Also note that for all the Mg exposure times [Fig. 3(c)], the C_3 shift is twice the one of C_2 and similar to the one of the low-energy cutoff. This demonstrates that the work function shift induced by Mg exposures is fully connected to an increased linear and downward band bending in the oxide film and that no bulk defects are present.

Therefore, we conclude that Mg exposures lead to the creation of positively charged donor-type electronic states at the oxide surface. The induced surface charges depend on the Mg exposure time and the linear band bending demonstrates that the electron transfer

occurs between the MgO surface and the metal substrate (Fig 4 (a), (b)). As demonstrated in electron paramagnetic resonance (EPR) experiments, deposition of small amounts of Mg at low temperatures on 20 ML-thick MgO(001) single crystalline films leads to creation of F_s^+ color centers.[17] Identically, we assign our Mg-induced donor-type surface states to F_s^+ color centers that have been shown to concern unpaired electrons trapped at morphological defects of the MgO surface. Next, assuming only F_s^+ centers of uniform surface density and a relative dielectric constant of 8.0 for MgO, a classical capacitor model can be used to estimate the amount of Mg-induced charged color centers. Considering a MgO thickness of 3 ML and a work function variation $\Delta\phi$ of -0.37 eV after 20 seconds of Mg exposure, the density of F_s^+ centers can be estimated to be $2.7\times10^{13}/\mathrm{cm}^2$.

Interestingly, the measured work function variation $\Delta\phi$ obtained for the 5ML-thick MgO film after 20 seconds of Mg exposure is identical to the one obtained for the MgO(3ML)/Ag(001) sample [Fig. 1]. This imply a lower density of F_s^+ centers induced on the 5ML-thick MgO film. It has been demonstrated that the ultrathin limit strongly impacts the stability of oxygen vacancies-induced F_s and F_s^+ centers on MgO/Ag(100).[24] In particular, the doubly occupied F_s center has been shown to be metastable with respect to the paramagnetic F_s^+ center thanks to favored charge transfer with the Ag substrate. Bearing in mind that the present Mg-induced band bending is linear and reflects electron charge transfer between the MgO surface and the metal substrate, we conclude that Mg exposures of ultrathin MgO/Ag(001) films lead to a controlled creation of surface F_s^+ centers which is enhanced by the ultrathin limit and associated tunneling effects.

The analogy between electron-induced (oxygen vacancies) and Mg-induced color centers is finally pushed forward through the surface reactivity of Mg-induced color centers with O_2. From the Mg $KL_{23}L_{23}$ Auger spectrum obtained after O_2 exposure (Fig. 3(b)), we indeed see that whereas the C_1 still does not exhibit energy shift, the C_2 and C_3 components appear at higher kinetic energy than the ones of the spectrum measured directly after Mg exposure. More precisely, the positive shifts of C_2 and C_3 correspond to a full cancellation of the Mg-

induced downward band bending (black curve in Fig. 3(c)), as observed by UPS [Fig. 2]. Thus, after the O_2 exposition, the charge transfer between the MgO surface and the metal substrate is close to the one of the as-grown sample. The exposition of the sample to an O_2 molecular atmosphere therefore induces an electron transfer from the interface towards the surface of the MgO/Ag(001) sample.

Theoretical work and EPR measurements have shown that activated molecular oxygen O_2^- (also called superoxide radical anions) form spontaneously on thin Mo-supported MgO(001) films for oxide thicknesses lower than 8 ML.[8,9] Also, it has been theoretically found that O_2^- anions (with -0.72e) form on MgO(2ML)/Ag(001)[7] by charge transfer from both the Ag substrate (0.18e) and the underlying MgO layer (0.54e) to the O_2 molecule. We can therefore expect that the adsorption and activation of molecular oxygen on terraces of MgO ultrathin films substantially reduces the band bending (giving an upward bending) of the MgO layer and increases the work function of the metal-dielectric system.

Besides, whereas O_2 molecules do not adsorb on regular MgO(001) surfaces of bulk monocrystals,[25] the presence of surface F_s and F_s^+ centers allows to create O_2^- surface species,[26] through the formation of O_2^-/F_s^+ and O_2^-/F_s^{2+} complexes by electron transfer from the color centers to the empty level of the adsorbed molecule.[27,28] We propose that such kind of complexes are also created at the surface of the MgO ultrathin film during the interaction of the colored MgO(001) surface with O_2. Their formation gives rise to an upward band-bending that demonstrates that an electron transfer from the metal to the complexes takes place during the exposure phase to molecular oxygen (Fig. 4 (b),(c)). The fact that MgO recovers the flat band condition implies that the surface is close to neutrality condition in the final stage (Fig. 4(c)).

Thus, as Mo-doped CaO,[29] or Au chains supported on MgO/Mo thin films,[10] we believe that our Mg-colored 3ML-thick MgO/Ag(001) system favors O_2 activation through an enhanced charge transfer mechanism between the oxide surface and the metal support. Further ab initio calculations should confirm our spectroscopic findings and provide a deeper

understanding of adsorption processes of O_2 on the low-coordinated surface sites of metal-supported MgO(001)ultrathin films.

Conclusion

To conclude, we probed charge transfer mechanisms acting at interfaces of Ag-supported ultrathin MgO films successively exposed to Mg and O_2 flux by photoemission spectroscopy and we reported evidence for controlled creation of Mg-induced color centers and catalytic enhancement of O_2 activation. Our findings give new insight for studying electronic properties of dielectric/metal systems such as work functions, defect states and Schottky barrier heights and their relationship to catalytic processes.

Acknowledgments

The authors warmly acknowledge A. Le Pottier for technical support. This work was partially supported by the Fonds National Suisse pour la Recherche Scientifique through Division II.

References

(1) Freund, H.-J.; Pacchioni, G. Oxide Ultra-Thin Films on Metals: New Materials for the Design of Supported Metal Catalysts. *Chem. Soc. Rev.* **2008**, *37*, 2224-2242.

(2) Surnev, S.; Fortunelli, A.; Netzer, F. P. Structure-Property Relationship and Chemical Aspects of Oxide-Metal Hybrid Nanostructures. *Chem. Rev.* **2013**, *113*, 4314-4372.

(3) Pacchioni, G.; Giordano, L.; Baistrocchi, M. Charging of Metal Atoms on Ultrathin MgO/Mo(100) Films. *Phys. Rev. Lett.* **2005** *94*, 226104.

(4) Sterrer, M.; Risse, T.; Martinez Pozzoni, U.; Giordano, L.; Heyde, M.; Rust, H.-P.;

Pacchioni, G.; Freund, H.-J. Control of the Charge State of Metal Atoms on Thin MgO Films. *Phys. Rev. Lett.* **2007**, *98*, 096107.

(5) Sterrer, M.; Risse, T.; Heyde, M.; Rust, H.-P.; Freund, H.-J. Crossover from Three-Dimensional to Two-Dimensional Geometries of Au Nanostructures on Thin MgO(001) Films: A Confirmation of Theoretical Predictions. *Phys. Rev. Lett.* **2007** *98*, 206103.

(6) Benedetti, S.; Stavale, F.; Valeri, S.; Noguera, C.; Freund, H.-J.; Goniakowski, J.; Nilius, N. Steering the Growth of Metal Ad-Particles via Interface Interactions Between an MgO Thin Film and a Mo(001) Support. *Adv. Funct. Mater.* **2013** *23*, 75-80.

(7) Hellman, A.; Klacar, S.; Grönbeck, H. Low Temperature CO Oxidation over Supported Ultrathin MgO Films. *J. Am. Chem. Soc.* **2009** *131*, 16636-16637.

(8) Gonchar, A.; Risse, T.; Freund, H.-J.; Giordano, L.; Di Valentin, C.; Pacchioni, G. Activation of Oxygen on MgO: O_2^- Radical Ion Formation on Thin, Metal-Supported MgO(001) Films. *Angew. Chem. Int. Ed.* **2011** *50*, 2635-2638.

(9) Song, Z.; Fan, J.; Shan, Y.; Ching Ng, A. M.; Xu, H. Generation of Highly Reactive Oxygen Species on Metal-Supported MgO(100) Thin Films. *Phys. Chem. Chem. Phys* **2016** *18*, 25373-25379.

(10) Frondelius, F.; Häkkinen, H.; Honkala, K. Adsorption and Activation of O_2 at Au Chains on MgO/Mo Thin Films. *Phys. Chem. Chem. Phys.* **2010** *12*, 1483-1492.

(11) Yoon, B.; Hakkinen, H.; Landman, U.; Worz, A. S.; Antonietti, J. M.; Abbet, S.; Judai, K.; Heiz, U. Charging Effects on Bonding and Catalyzed Oxidation of CO on Au_8 Clusters on MgO. *Science* **2005** *307*, 403-407.

(12) Sanchez, A.; Abbet, S.; Heiz, U.; Schneider, W. D.; Häkkinen, H.; Barnett, R. N.; Landmann, U. When Gold Is Not Noble: Nanoscale Gold Catalysts. *Phys. Chem. A* **1999** *103*, 9573-9578.

(13) Abbet, S.; Sanchez, A.; Heiz, U.; Schneider, W. D.; Ferrari, A.; Pacchioni, G.; Rösch, N. Acetylene Cyclotrimerization on Supported Size-Selected Pd_n Clusters ($1 \leq n \leq 30$): One Atom is Enough!. *J. Am. Chem. Soc.* **2000** *122*, 3453-3457.

(14) Abbet, S.; Riedo, E.; Brune, H.; Heiz, U.; Ferrari, A. M.; Giordano, L.; Pacchioni, G. Identification of Defect Sites on MgO(100) Thin Films by Decoration with Pd Atoms and Studying CO Adsorption Properties. *J. Am. Chem. Soc.* **2001** *123*, 6172-6178.

(15) Moseler, M.; Häkkinen, H.; Landmann, U. Supported Magnetic Nanoclusters: Soft Landing of Pd Clusters on a MgO Surface. *Phys. Rev. Lett.* **2002** *89*, 176103.

(16) Giordano, L.; Di Valentin, C.; Goniakowski, J.; Pacchioni, G. Nucleation of Pd Dimers at Defect Sites of the MgO(100) Surface. *Phys. Rev. Lett.* **2004** *92*, 096105.

(17) Gonchar A.; Risse, T.; Giamello, E.; Freund, H.-J. Additive Coloring of Thin, Single Crystalline MgO(001) Films. *Phys. Chem. Chem. Phys.* **2010** *12*, 12520-12524.

(18) Sterrer, M.; Fischbach, E.; Heyde, M.; Nilius, N.; Rust, H.-P.; Risse, T.; Freund, H.J. Electron Paramagnetic Resonance and Scanning Tunneling Microscopy Investigations on the Formation of F^+ and F^0 Color Centers on the Surface of Thin MgO(001) Films. *J. Phys. Chem. B* **2006** *110*, 8665-8669.

(19) Jaouen, T.; Jézéquel, G.; Delhaye, G.; Lépine, B.; Turban, P.; Schieffer, P. Work Function Shifts, Schottky Barrier Height, and Ionization Potential Determination of Thin MgO Films on Ag(001). *Appl. Phys. Lett.* **2010** *97*, 232104.

(20) Jaouen, T.; Tricot, S.; Delhaye, G.; Lépine, B.; Sébilleau, D.; Jézéquel, G.; Schieffer, P. Layer-Resolved Study of Mg Atom Incorporation at the MgO/Ag(001) Buried Interface. *Phys. Rev. Lett.* **2013** *111*, 027601.

(21) Tjeng, L. H.; Vos, A. R.; Sawatzky, G. A. Electronic Structure of MgO Studied by Angle-Resolved Ultraviolet Photoelectron Spectroscopy. *Surf. Sci.* **1990** *235*, 269-279.

(22) Jaouen, T.; Aebi, P.; Tricot, S.; Delhaye, G.; Lépine, B.; Sébilleau, D.; Jézéquel, G.; Schieffer, P. Induced Work Function Changes at Mg-Doped MgO/Ag(001) Interfaces: Combined Auger Electron Diffraction and Density Functional Study. *Phys. Rev. B* **2014** *90*, 125433.

(23) Jaouen, T.; Razzoli, E.; Didiot, C.; Monney, G.; Hildebrand, B.; Vanini, F.; Muntwiler, M.; Aebi, P. Excited States at Interfaces of a Metal-Supported Ultrathin Oxide Film. *Phys. Rev. B* **2015** *91*, 161410(R).

(24) Giordano, L.; Martinez, U.; Pacchioni, G.; Watkins, M.; Shluger, A. L. F and F^+ Centers on MgO/Ag(100) or MgO/Mo(100) Ultrathin Films: Are They Stable?. *J. Phys. Chem. C* **2008** *112*, 3857-3865.

(25) Kantorovich, L. N.; Gillan, M. J. Adsorption of Atomic and Molecular Oxygen on the MgO(001) Surface. *Surf. Sci.* **1997** *374*, 373-386.

(26) Giamello, E.; Ferrero, A.; Collucia, S.; Zecchina, A. Defect Centers Induced by Evaporation of Alkali and Alkaline-Earth Metals on Magnesium Oxide: An EPR Study. *J. Phys. Chem.* **1991** *95*, 9385-9391.

(27) Ferrari, A. M.; Pacchioni, G. Surface Reactivity of MgO Oxygen Vacancies: Electrostatic Mechanisms in the Formation of O_2^- and CO^- Species. *J. Chem. Phys.* **1997** *107*, 2066-2078.

(28) Pacchioni, G.; Ferrari, A. M. Surface Reactivity of MgO Oxygen Vacancies. *Catalysis Today* **1999** *50*, 533-540.

(29) Cui, Y.; Shao, X.; Baldofski, M.; Sauer, J.; Nilius, N.; Freund, H.-J. Adsorption, Activation, and Dissociation of Oxygen on Doped Oxides. *Angew. Chem. Int. Ed.* **2013** *52*, 11385-11387.

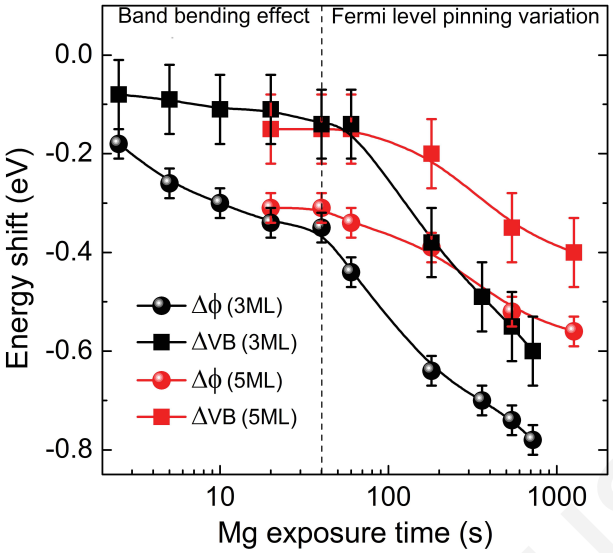

Figure 1: Variations of the work function $\Delta\phi$ and MgO-valence band position ΔVB as a function of the Mg exposure time for 3 ML MgO/Ag(001) (black lines) and 5 ML MgO/Ag(001) (red lines) samples. The evolutions are plotted in semi-logarithmic representation.

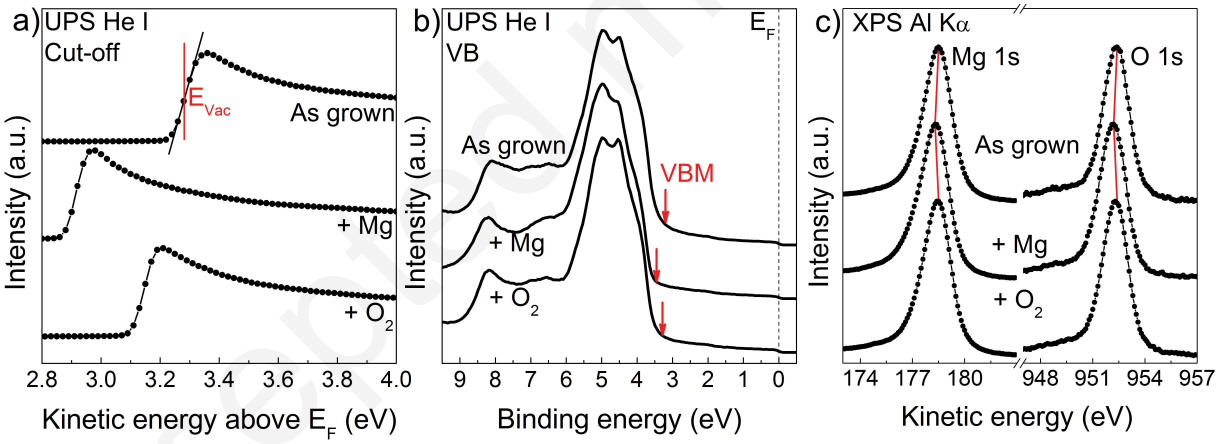

Figure 2: (a) Low-energy cutoff of the secondary photoelectrons emission for the MgO(3ML)/Ag(001) sample (top) and after successive exposures to a Mg (middle) and O_2 (bottom) flux. The Mg and O_2 exposures have been performed during 20 s and 240 s, respectively. The energy reference is taken at E_F and the low-energy cutoff positions were taken at the maximum slope of their rising edges as indicated on the top spectrum.(b) He-I UPS spectra showing the valence band region of the MgO reference sample (top) and after Mg (middle) and O_2 exposures (bottom). The energy reference is taken at the Fermi level E_F. The VBM positions are indicated by the red arrows. (c) Al $K\alpha$ spectra of the Mg $1s$ and O $1s$ core levels of the MgO reference sample (top) and after Mg (middle) and O_2 exposures (bottom). The red lines indicate the induced core level shifts.

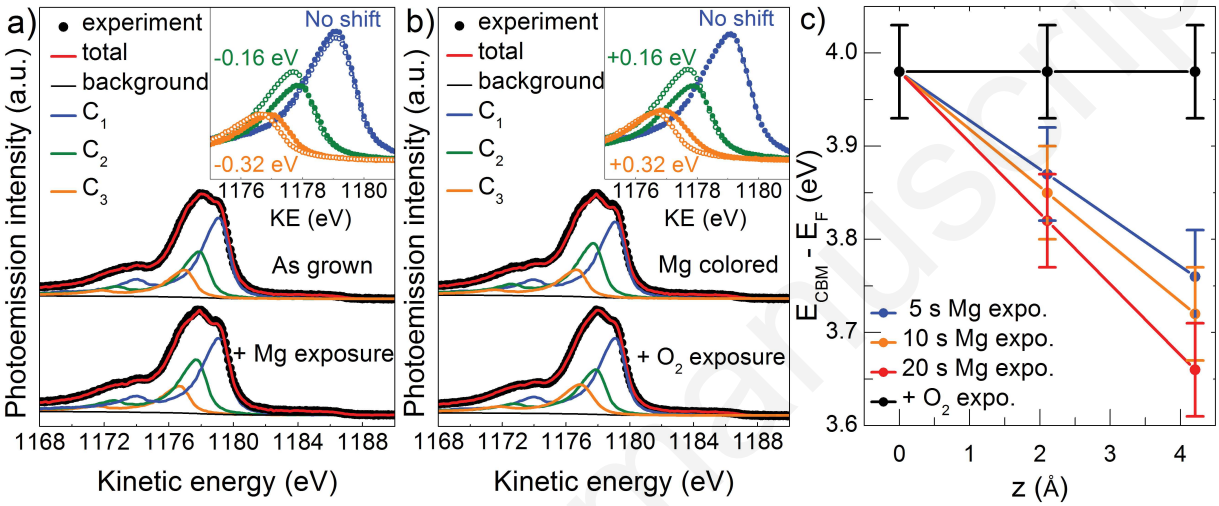

Figure 3: (a) Photoemission spectra of the Mg $KL_{23}L_{23}$ Auger transition of the as-grown (top) and Mg-exposed (bottom) 3 ML-thick MgO samples. The inset shows the interface (C_1), subsurface (C_2) and surface Auger (C_3) components of the fitted Auger spectra obtained on the reference (full markers) and Mg-exposed (empty markers) samples. (b) Photoemission spectra of the Mg $KL_{23}L_{23}$ Auger transition of the 3 ML Mg-exposed MgO film before (top) and after (bottom) O_2 exposure. The inset shows the interface (C_1), subsurface (C_2) and surface Auger (C_3) components of the fitted Auger spectra obtained on the Mg-colored (empty markers) and O_2-exposed (full markers) samples. Best fit and layer-by-layer decomposition are also shown. (c) Evolution of the band bending through the MgO oxide layer extracted from the layer-resolved photoemission measurements for the different Mg exposure times and after O_2 exposure (black line). The position of the conduction band minimum (CBM) with respect to the Fermi level is taken as reference. The 3 ML MgO/Ag(001) clean sample is initially considered to be in flat-band condition.

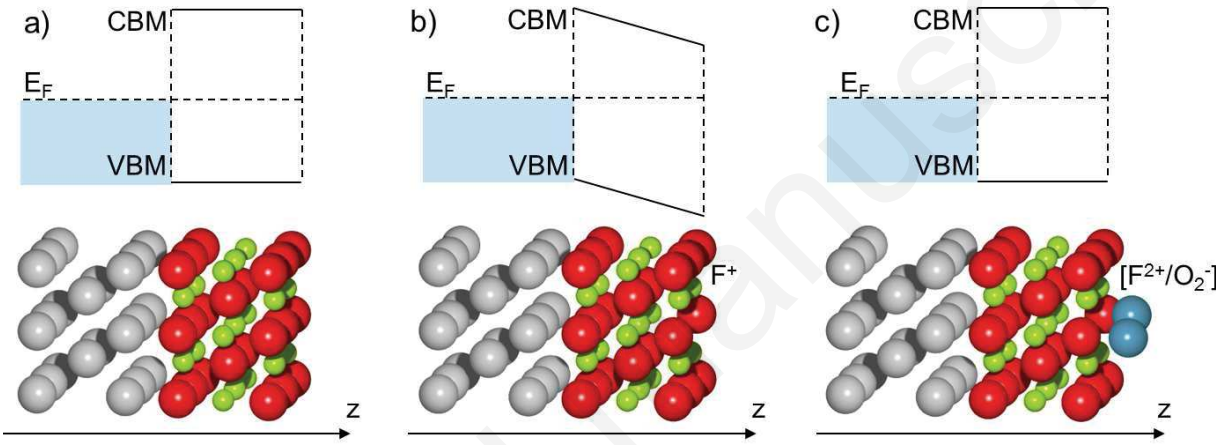

Figure 4: Schematic band diagrams of the MgO(3ML)/Ag(001) as-grown sample (a), and after Mg (b) and O_2 exposures (c). The as-grown sample is initially considered to be in flat-band condition. The Mg exposure results in F^+ center creation at the MgO surface and in a downward band bending (b), whereas the O_2 exposure leads to $[F^{2+}/O_2^-]$ complexes formation that gives rise to an upward band bending indicating an electron transfer from the metal to the complexes (c). E_F, VBM, and CBM respectively stand for Ag Fermi level, valence band maximum, and conduction band minimum. The red, green and gray atoms correspond to oxygen, magnesium and silver, respectively. The O_2 molecule involved in the $[F^{2+}/O_2^-]$ complex is shown in blue.

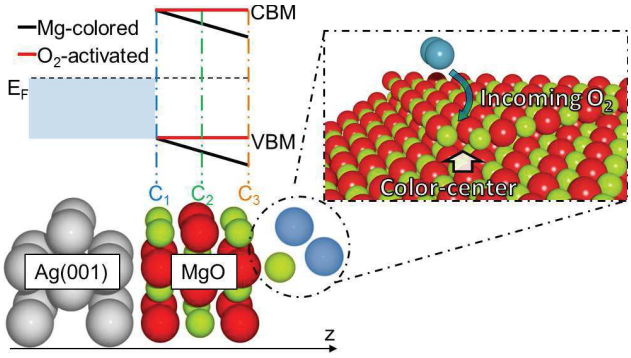

TOC Graphic